SUPPLEMENTARY INFORMATION TO:

New particle formation from sulfuric acid and ammonia: nucleation and growth model based on thermodynamics derived from CLOUD measurements for a wide range of conditions

Andreas Kürten

Institute for Atmospheric and Environmental Sciences, Goethe University Frankfurt, 60438 Frankfurt am Main, Germany.

SI Text1: Acid-base model differential equations

The model integrates the differential equations listed below using a fourth-order Runge-Kutta algorithm. The time-dependent concentration for each cluster depends on the balance between production rate, P, and loss rate, L. Relevant loss terms in the present study (analyzing new particle formation in the CLOUD chamber) are the wall loss rate, k_w, the dilution rate, k_{dil}, and the condensation/coagulation sink (see Kürten et al., 2018). For the smallest clusters the evaporation rate, E, is also a relevant loss process. The clusters in the molecular size bins are denoted by their sulfuric acid content, A, where an index indicates the number of molecules contained in the cluster. For the smallest clusters (monomer up to the tetramer) the clusters are also distinguished according to their base content, where B with an index indicates the number of base (ammonia) molecules in the cluster (note that the clusters never contain more base than acid, see main text). This nomenclature results in the following set of equations.

Monomers (A_1 and A_1B_1):

$$\frac{dA_1B_1}{dt} = P - L \cdot A_1B_1 \tag{1a}$$

$$P = K_{1,1} \cdot A_1 \cdot B_1 + E_{A2B1} \cdot A_2B_1 \tag{1b}$$

$$L = k_{w,1} + k_{dil} + E_{A1B1} + \sum_{i=1}^{n} K_{1,i} \cdot N_i \tag{1c}$$

The last term in the equation of the losses (L) represents the condensation/coagulation sink.

The parameter $A_{1,total}$ is a constant input parameter determining the total sulfuric acid concentration. From this the concentration of "free" sulfuric acid is calculated in every time step of the integration:

$$A_1 = A_{1,total} - A_1B_1 \tag{1d}$$

Dimers (A_2, A_2B_1 and A_2B_2):

$$\frac{dA_2}{dt} = P - L \cdot A_2 \tag{2a}$$

$$P = 0.5 \cdot K_{1,1} \cdot A_1 \cdot A_1 + E_{A3B0} \cdot A_3 \tag{2b}$$

$$L = k_{w,2} + k_{dil} + E_{A2} + K_{1,2} \cdot B_1 + \sum_{i=1}^{n} K_{2,i} \cdot N_i \tag{2c}$$

$$\frac{dA_2B_1}{dt} = P - L \cdot A_2B_1 \tag{2d}$$

$$P = K_{1,1} \cdot A_1 \cdot A_1B_1 + K_{1,2} \cdot B_1 \cdot A_2 + E_{A2B2} \cdot A_2B_2 + E_{A3B1} \cdot A_3B_1 \tag{2e}$$

$$L = k_{w,2} + k_{dil} + E_{A2B1} + K_{1,2} \cdot B_1 + \sum_{i=1}^{n} K_{2,i} \cdot N_i \tag{2f}$$

$$\frac{dA_2B_2}{dt} = P - L \cdot A_2B_2 \tag{2g}$$

$$P = 0.5 \cdot K_{1,1} \cdot A_1B_1 \cdot A_1B_1 + K_{1,2} \cdot B_1 \cdot A_2B_1 + E_{A3B2} \cdot A_3B_2 \tag{2h}$$

$$L = k_{w,2} + k_{dil} + E_{A2B2} + \sum_{i=1}^{n} K_{2,i} \cdot N_i \tag{2i}$$

Trimers (A_3, A_3B_1, A_3B_2 and A_3B_3):

$$\frac{dA_3}{dt} = P - L \cdot A_3 \tag{3a}$$

$$P = K_{1,2} \cdot A_1 \cdot A_2 + E_{A4} \cdot A_4 \tag{3b}$$

$$L = k_{w,3} + k_{dil} + E_{A3} + K_{1,3} \cdot B_1 + \sum_{i=1}^{n} K_{3,i} \cdot N_i \tag{3c}$$

$$\frac{dA_3B_1}{dt} = P - L \cdot A_3B_1 \tag{3d}$$

$$P = K_{1,2} \cdot A_1 \cdot A_2B_1 + K_{1,3} \cdot B_1 \cdot A_3 + K_{1,2} \cdot A_1B_1 \cdot A_2 + E_{A4B1} \cdot A_4B_1 \tag{3e}$$

$$L = k_{w,3} + k_{dil} + E_{A3B1} + K_{1,3} \cdot B_1 + \sum_{i=1}^{n} K_{3,i} \cdot N_i \tag{3f}$$

$$\frac{dA_3B_2}{dt} = P - L \cdot A_3B_2 \tag{3g}$$

$$P = K_{1,3} \cdot B_1 \cdot A_3B_1 + K_{1,2} \cdot A_1 \cdot A_2B_2 + K_{1,2} \cdot A_1B_1 \cdot A_2B_1 + E_{A4B2} \cdot A_4B_2 + E_{A3B3} \cdot A_3B_3 \tag{3h}$$

$$L = k_{w,3} + k_{dil} + E_{A3B2} + K_{1,3} \cdot B_1 + \sum_{i=1}^{n} K_{3,i} \cdot N_i \tag{3i}$$

$$\frac{dA_3B_3}{dt} = P - L \cdot A_3B_3 \tag{3j}$$

$$P = K_{1,3} \cdot B_1 \cdot A_3B_2 + K_{1,2} \cdot A_1B_1 \cdot A_2B_2 + E_{A4B3} \cdot A_4B_3 \tag{3k}$$

$$L = k_{w,3} + k_{dil} + E_{A3B3} + \sum_{i=1}^{n} K_{3,i} \cdot N_i \tag{3l}$$

Tetramers (A_4, A_4B_1, A_4B_2, A_4B_3 and A_4B_4):

$$\frac{dA_4}{dt} = P - L \cdot A_4 \qquad (4a)$$

$$P = K_{1,3} \cdot A_1 \cdot A_3 + 0.5 \cdot K_{2,2} \cdot A_2 \cdot A_2 \qquad (4b)$$

$$L = k_{w,4} + k_{dil} + E_{A4} + K_{1,4} \cdot B_1 + \sum_{i=1}^{n} K_{4,i} \cdot N_i \qquad (4c)$$

$$\frac{dA_4B_1}{dt} = P - L \cdot A_4B_1 \qquad (4d)$$

$$P = K_{1,4} \cdot B_1 \cdot A_4 + K_{1,3} \cdot A_1 \cdot A_3B_1 + K_{1,3} \cdot A_1B_1 \cdot A_3 + K_{2,2} \cdot A_2 \cdot A_2B_1 \qquad (4e)$$

$$L = k_{w,4} + k_{dil} + E_{A4B1} + K_{1,4} \cdot B_1 + \sum_{i=1}^{n} K_{4,i} \cdot N_i \qquad (4f)$$

$$\frac{dA_4B_2}{dt} = P - L \cdot A_4B_2 \qquad (4g)$$

$$P = K_{1,4} \cdot B_1 \cdot A_4B_1 + K_{1,3} \cdot A_1 \cdot A_3B_2 + K_{1,3} \cdot A_1B_1 \cdot A_3B_1 + K_{2,2} \cdot A_2 \cdot A_2B_2 + 0.5 \cdot K_{2,2} \cdot A_2B_1 \cdot A_2B_1 \qquad (4h)$$

$$L = k_{w,4} + k_{dil} + E_{A4B2} + K_{1,4} \cdot B_1 + \sum_{i=1}^{n} K_{4,i} \cdot N_i \qquad (4i)$$

$$\frac{dA_4B_3}{dt} = P - L \cdot A_4B_3 \qquad (4j)$$

$$P = K_{1,4} \cdot B_1 \cdot A_4B_2 + K_{1,3} \cdot A_1 \cdot A_3B_3 + K_{1,3} \cdot A_1B_1 \cdot A_3B_2 + K_{2,2} \cdot A_2B_1 \cdot A_2B_2 + E_{A4B4} \cdot A_4B_4 \qquad (4k)$$

$$L = k_{w,4} + k_{dil} + E_{A4B3} + K_{1,4} \cdot B_1 + \sum_{i=1}^{n} K_{4,i} \cdot N_i \, CS_{A4B3} \qquad (4l)$$

$$\frac{dA_4B_4}{dt} = P - L \cdot A_4B_4 \qquad (4m)$$

$$P = K_{1,4} \cdot B_1 \cdot A_4B_3 + K_{1,3} \cdot A_1B_1 \cdot A_3B_3 + 0.5 \cdot K_{2,2} \cdot A_2B_2 \cdot A_2B_2 \qquad (4n)$$

$$L = k_{w,4} + k_{dil} + E_{A4B4} + \sum_{i=1}^{n} K_{4,i} \cdot N_i \qquad (4o)$$

From the concentrations of the acid-base clusters the concentrations of the total monomer (N_1), dimer (N_2), trimer (N_3) and tetramer (N_4) can be determined:

$$N_1 = A_1 + A_1 B_1 \quad (5a)$$

$$N_2 = A_2 + A_2 B_1 + A_2 B_2 \quad (5b)$$

$$N_3 = A_3 + A_3 B_1 + A_3 B_2 + A_3 B_3 \quad (5c)$$

$$N_4 = A_4 + A_4 B_1 + A_4 B_2 + A_4 B_3 + A_4 B_4 \quad (5d)$$

The calculation of the larger clusters (starting with the pentamer) and particles is calculated in the same way as described previously (Kürten et al., 2018):

$$\frac{dN_{k\geq 5}}{dt} = P - L \cdot N_{k\geq 5} \quad (5e)$$

$$P = \frac{1}{2} \cdot \sum_{i+j=k} \cdot N_i \cdot N_j \quad (5f)$$

$$L = k_{w,k} + k_{dil} + \sum_{j=1}^{n} K_{k,j} \cdot N_j \quad (5g)$$

SI Text2: Calculation of evaporation rates

Evaporation rates are calculated from dH (in kcal mol^{-1}) and dS (in cal mol^{-1} K^{-1}) according to (Ortega et al., 2012, Kürten et al., 2015):

$$E = \frac{K \cdot 10^{-6}}{k_B \cdot T \cdot K_{eq}}. \quad (6)$$

The equilibrium constant, K_{eq}, is given by

$$K_{eq} = \frac{1}{10^5\ Pa} \cdot exp\left(-\frac{dH \cdot 1000}{R'_{gas} \cdot T} + \frac{dS}{R'_{gas}}\right). \quad (7)$$

The constants are k_B = 1.381×10^{23} J K^{-1} and R_{gas}' = 1.987 cal mol^{-1} K^{-1}; T is the temperature and K the collision rate constant (Chan and Mozurkewich, 2001); the scaling factor 10^6 is used to convert the collision constant from cm^3 s^{-1} to m^3 s^{-1}.

SI FIGURES

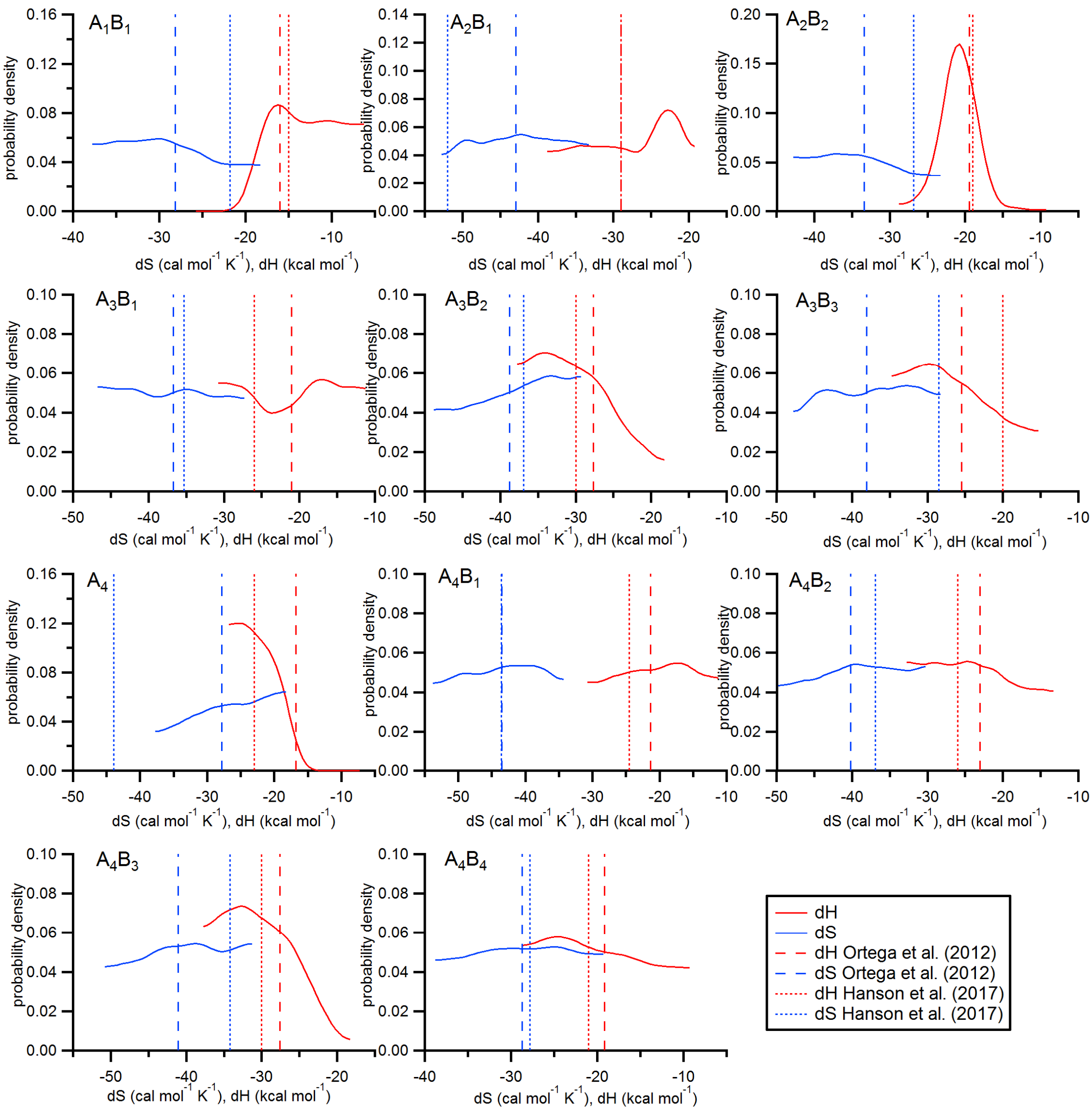

Figure S1: Probability density functions of dH and dS values for 11 clusters in the acid base system (A_xB_y = cluster of sulfuric acid and ammonia with x sulfuric acid molecules and y ammonia molecules). The solid curves show the results from the Monte Carlo simulation. The vertical lines indicate the literature data from Ortega et al. (2012, dashed lines) and Hanson et al. (2017, dotted lines).

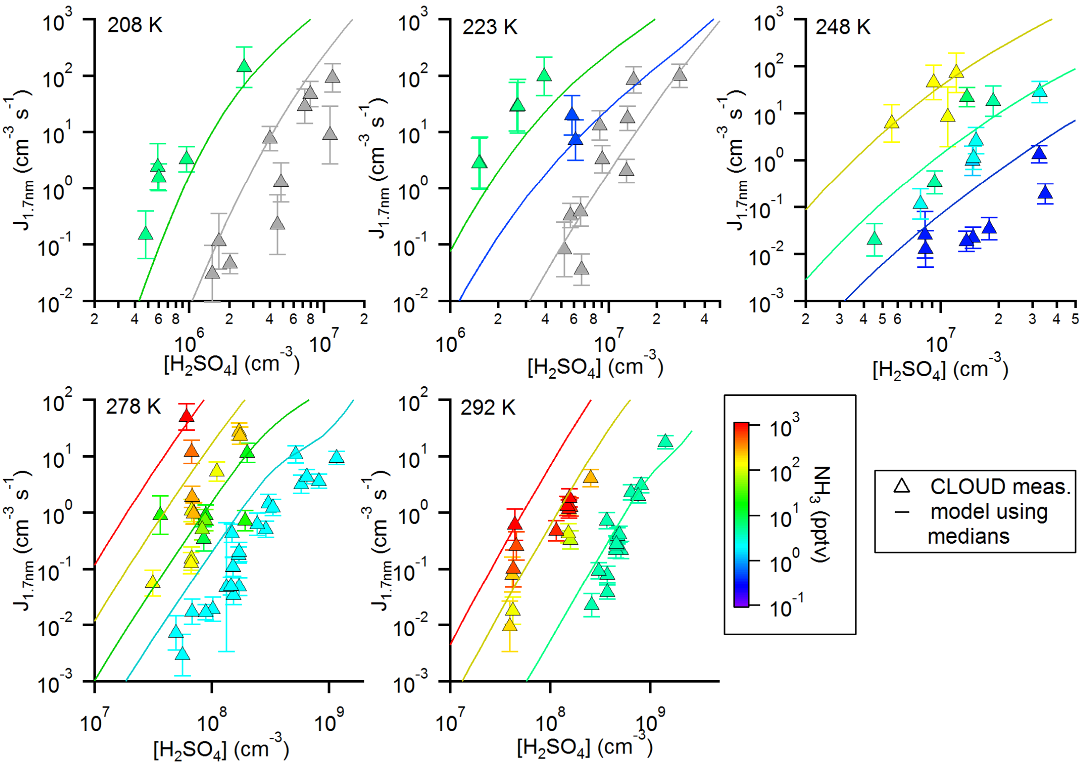

179
180
181 **Figure S2:** Comparison between simulated and measured new particle formation rates for five
182 different temperatures. The color code indicates the ammonia mixing ratio; the grey symbols
183 indicate pure binary conditions. The model uses the median values from Table 1 as the
184 thermodynamic data (see also Figure 2).

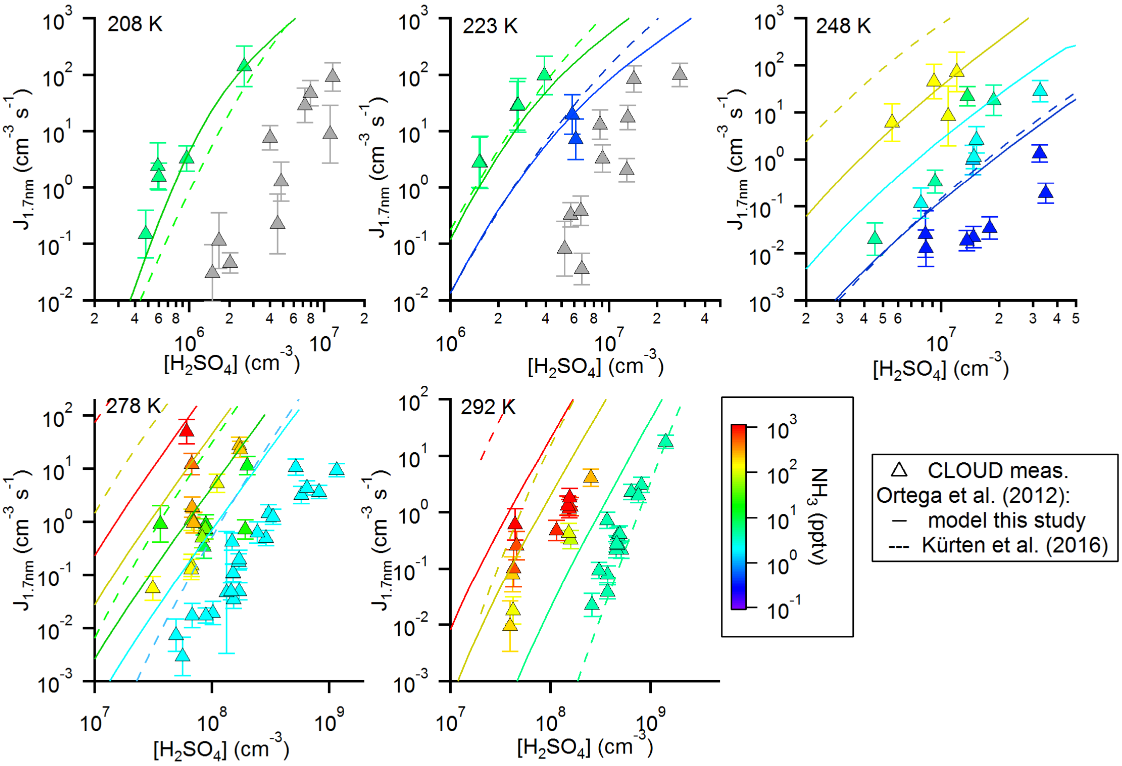

Figure S3: Comparison between simulated and measured new particle formation rates for five different temperatures. The color code indicates the ammonia mixing ratio; the grey symbols indicate pure binary conditions. The solid lines show results for the thermodynamic data from Ortega et al. (2012) implemented in the model of the present study. The dashed lines show the calculated NPF rates published previously by using the ACDC model with the same thermodynamic data (Kürten et al., 2016).

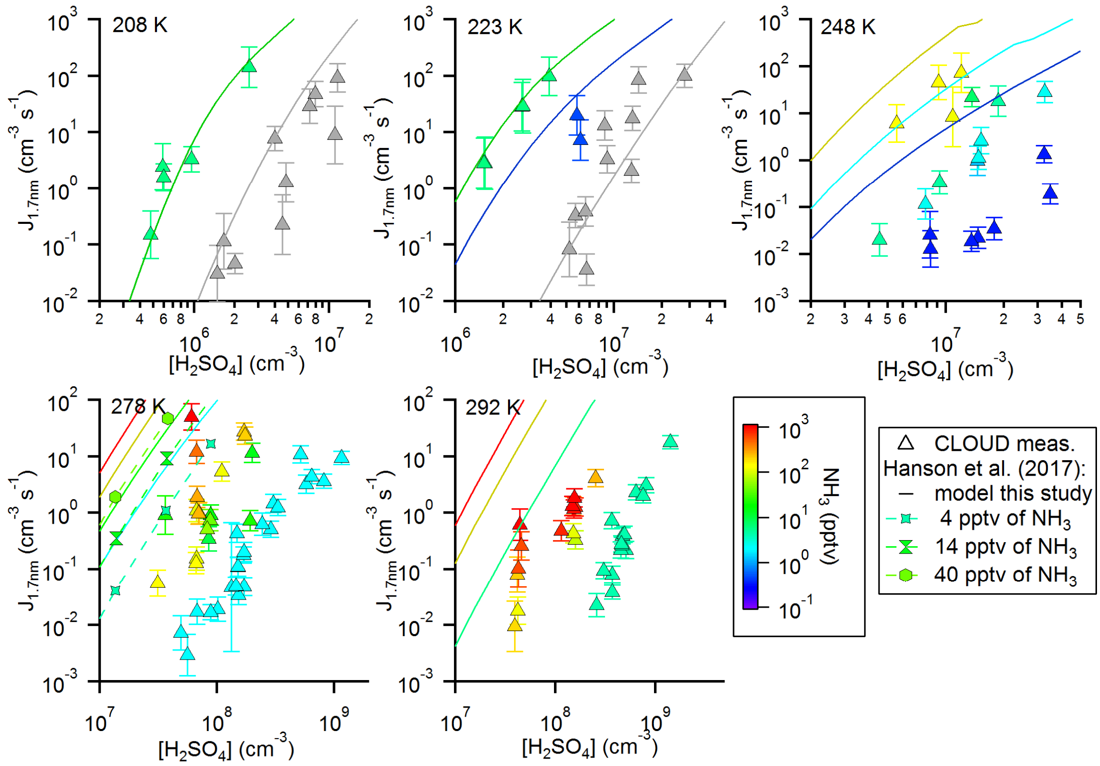

Figure S4: Comparison between simulated and measured new particle formation rates for five different temperatures. The color code indicates the ammonia mixing ratio; the grey symbols indicate pure binary conditions. The model uses thermodynamic data from Hanson et al. (2017). The symbols (stars, hourglass symbols and hexagons) at 278 K are original data taken from Hanson et al. (2017).

SI REFERENCES

Chan, T. W., and Mozurkewich, M.: Measurement of the coagulation rate constant for sulfuric acid particles as a function of particle size using tandem differential mobility analysis, *J. Aerosol Sci.*, 32, 321–339, doi: 10.1016/S0021-8502(00)00081-1, 2001.

Hanson, D. R., Bier, I., Panta, B., Jen, C. N., and McMurry, P. H.: Computational Fluid Dynamics Studies of a Flow Reactor: Free Energies of Clusters of Sulfuric Acid with NH_3 or Dimethyl Amine, *J. Phys. Chem. A*, 121, 3976−3990, doi: 10.1021/acs.jpca.7b00252, 2017.

Kürten, A., Münch, S., Rondo, L., Bianchi, F., Duplissy, J., Jokinen, T., Junninen, H., Sarnela, N. Schobesberger, S., Simon, M., Sipilä, M. Almeida, J., Amorim, A., Dommen, J., Donahue, N. M., Dunne, M., Flagan, R. C., Franchin, A., Kirkby, J., Kupc, A., Makhmutov, V., Petäjä, T. Praplan, A. P., Riccobono, F., Steiner, G., Tomé, A., Tsagkogeorgas, G., Wagner, P. E., Wimmer, D., Baltensperger, U., Kulmala, M., Worsnop, D. R., and Curtius, J.: Thermodynamics of the formation of sulfuric acid dimers in the binary (H_2SO_4-H_2O) and ternary (H_2SO_4-H_2O-NH_3) system, *Atmos. Chem. Phys.*, 15, 10701–10721, doi: 10.5194/acp-15-10701-2015, 2015.

Kürten, A., Bianchi, F., Almeida, J., Kupiainen-Määttä, O., Dunne, E. M., Duplissy, J., Williamson, C., Barmet, P., Breitenlechner, M., Dommen, J., Donahue, N. M., Flagan, R. C., Franchin, A., Gordon, H., Hakala, J., Hansel, A., Heinritzi, M., Ickes, L., Jokinen, T., Kangasluoma, J., Kim, J., Kirkby, J., Kupc, A., Lehtipalo, K., Leiminger, M., Makhmutov, V., Onnela, A., Ortega, I. K., Petäjä, T., Praplan, A. P., Riccobono, F., Rissanen, M. P., Rondo, L., Schnitzhofer, R., Schobesberger, S., Smith, J. N., Steiner, G., Stozhkov, Y., Tomé, A., Tröstl, J., Tsagkogeorgas, G., Wagner, P. E., Wimmer, D., Ye, P., Baltensperger, U., Carslaw, K., Kulmala, M., and Curtius, J.: Experimental particle formation rates spanning tropospheric sulfuric acid and ammonia abundances, ion production rates and temperatures, *J. Geophys. Res.-Atmos.*, 121, 12377–12400, doi: 10.1002/2015JD023908, 2016.

Kürten, A., Li, C., Bianchi, F., Curtius, J., Dias, A., Donahue, N. M., Duplissy, J., Flagan, R. C., Hakala, J., Jokinen, T., Kirkby, J., Kulmala, M., Laaksonen, A., Lehtipalo, K., Makhmutov, V., Onnela, A., Rissanen, M. P., Simon, M., Sipilä, M., Stozhkov, Y., Tröstl, J., Ye, P., and McMurry, P. H.: New particle formation in the sulfuric acid–dimethylamine–water system: reevaluation of CLOUD chamber measurements and comparison to an aerosol nucleation and growth model, *Atmos. Chem. Phys.*, 18, 845–863, doi: 10.5194/acp-18-845-2018, 2018.

Ortega, I. K., Kupiainen, O., Kurtén, T., Olenius, T., Wilkman, O., McGrath, M. J., Loukonen, V., and Vehkamäki, H.: From quantum chemical formation free energies to evaporation rates, *Atmos. Chem. Phys.*, 12, 225–235, doi: 10.5194/acp-12-225-2012, 2012.